

## Space-charge effects in photovoltaic double barrier quantum well infrared detectors

H. Schneider, E. C. Larkins, J. D. Ralston, K. Schwarz, F. Fuchs, and P. Koidl

Citation: [Applied Physics Letters](#) **63**, 782 (1993); doi: 10.1063/1.109906

View online: <http://dx.doi.org/10.1063/1.109906>

View Table of Contents: <http://scitation.aip.org/content/aip/journal/apl/63/6?ver=pdfcov>

Published by the [AIP Publishing](#)

---

### Articles you may be interested in

[Space-charge electric field in photorefractive multiple quantum wells](#)

Appl. Phys. Lett. **96**, 152106 (2010); 10.1063/1.3367728

[Correlation between the performance of double-barrier quantum-well infrared photodetectors and their microstructure: On the origin of the photovoltaic effect](#)

J. Appl. Phys. **98**, 044510 (2005); 10.1063/1.2006990

[Coupling effects observed in the intersubband photocurrent of photovoltaic double-barrier quantum-well infrared detectors](#)

J. Appl. Phys. **79**, 9369 (1996); 10.1063/1.362615

[Space-charge behavior near implanted contacts on infrared detectors](#)

J. Appl. Phys. **64**, 2153 (1988); 10.1063/1.341728

[Photovoltaic quantum well infrared detector](#)

Appl. Phys. Lett. **52**, 1701 (1988); 10.1063/1.99022

---

The image shows the cover of the journal Applied Physics Reviews. It features a 3D molecular model of a crystal lattice in shades of blue and white. The AIP logo and the journal title 'Applied Physics Reviews' are at the top. The cover also displays a diagram of a quantum well structure and some data plots.

## NEW Special Topic Sections

**NOW ONLINE**  
Lithium Niobate Properties and Applications:  
Reviews of Emerging Trends

**AIP** | Applied Physics  
Reviews

# Space-charge effects in photovoltaic double barrier quantum well infrared detectors

H. Schneider, E. C. Larkins, J. D. Ralston, K. Schwarz, F. Fuchs, and P. Koidl  
 Fraunhofer-Institut für Angewandte Festkörperphysik, Tullastraße 72, D-79108 Freiburg, Germany

(Received 7 August 1992; accepted for publication 26 May 1993)

We show that the spatial distribution of the dopants strongly influences the transport asymmetry and the photovoltage observed in double barrier quantum well intersubband photodetectors. This influence can be quantitatively explained by the local space-charge fields arising from an asymmetry of the doping profile with respect to the well centers. The resulting transport model correctly predicts *both* the observed transport asymmetry of the photocurrent and the opposite asymmetry of the dark current.

Intersubband transitions in quantum wells (QW) are of increasing importance for applications in infrared photodetectors.<sup>1-5</sup> Optimization of such devices requires a thorough understanding of the carrier transport in the barrier regions, of the carrier emission and capture by the QWs, and of carrier injection at the contacts.<sup>6</sup> Introducing double barrier quantum wells (DBQW), i.e., incorporating thin tunnel barriers between the wells and barriers of a multiple QW, provides an additional degree of freedom which can be used to separate and to modify the carrier capture and emission processes responsible for the detector operation.<sup>7,8</sup> Photovoltaic QW detectors are promising for practical applications, since the suppression of the dark current strongly improves the noise properties.<sup>8</sup>

Using these DBQW structures, we have systematically varied the location of the doped region relative to the QW layers. In this letter we show that the photovoltaic behavior of the DBQW detectors is very sensitive to the exact position of the dopant layer. This dependence is quantitatively explained by a simple model which uses the Poisson equation. Based on these results, we propose a transport model which predicts the observed photovoltaic behavior *and* explains why the observed asymmetry of the photocurrent is opposite to that of the dark current.

The samples used in this work are 50 period DBQW structures consisting of 5 nm Si-doped GaAs wells, sandwiched between 2 nm thick AlAs tunnel barriers, and further separated by 25 nm Al<sub>0.3</sub>Ga<sub>0.7</sub>As layers. Three samples are studied here, with the intended positions of the nominally 4 nm wide Si doping spikes (dopant concentration of  $2 \times 10^{18} \text{ cm}^{-3}$ ) in the 5 nm wide GaAs QWs shown in the lower inset of Fig. 1. Si-doped GaAs contact layers ( $1 \times 10^{18} \text{ cm}^{-3}$ ) with thicknesses of 0.5 and 1.0  $\mu\text{m}$  were included above and below the active region, respectively. The structures were grown at 580 °C by molecular-beam epitaxy on (100)-oriented semi-insulating GaAs (liquid-encapsulated Czochralski) substrates and processed into mesa detectors of the 0.04 mm<sup>2</sup> are with ring-shaped ohmic contacts. Photocurrent was excited using a glowbar. Photocurrent spectra recorded with a Fourier spectrometer showed peak energies of  $2390 \pm 30 \text{ cm}^{-1}$  with a full width at half maximum of typically  $230 \text{ cm}^{-1}$ . The measured line shape of the photocurrent spectra was insensitive to the applied voltage. The voltage dependence of the integrated

photocurrent intensity was measured using lock-in techniques and broadband illumination.

Figure 1 shows the dependence of the photocurrent of the three samples on the voltage applied to the top contact. All three structures show a photovoltaic behavior (i.e., a steady-state photocurrent at 0 V bias, resulting in a photovoltage under open-circuit conditions). The polarity of this photovoltage indicates transport of the photoexcited electron predominantly towards the substrate. An upper limit for this photovoltage is given by the *internal flatband condition*, defined as the external voltage  $V_N$  where the photocurrent vanishes. This definition is analogous to that of the built-in voltage of a *p-n* junction photodiode. We point out that the measured  $V_N$  does not depend on the illumination density. Thus,  $V_N$  is a useful figure of merit for photovoltaic intersubband detectors. In Fig. 1,  $V_N$  varies systematically with the position of the doping spike. Since  $V_N$  is the only parameter which will be discussed in the following, we did not determine the precise value of the photocurrent responsivity. The reproducibility of the intersubband excitation density between the different samples is estimated to be better than 90%.

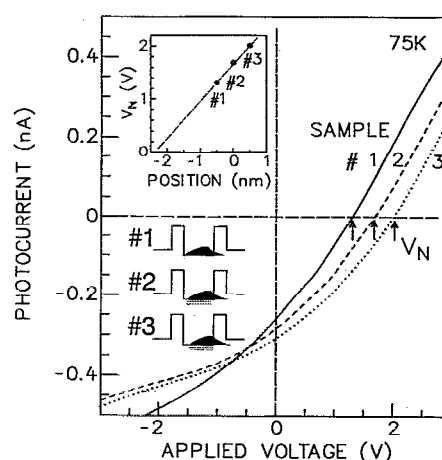


FIG. 1. Photocurrent vs applied voltage of the DBQW detectors. Negative photocurrent corresponds to electron transport towards the substrate side. Lower inset: Spatial dependence of the conduction band edge. The shaded and black areas represent the intended position of the Si doping spike and a realistic dopant distribution, respectively. Growth direction is from the left to the right. Upper inset: Flatband voltage  $V_N$  vs relative doping position.

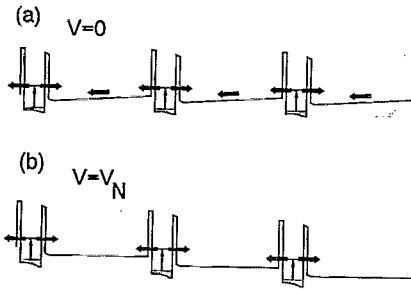


FIG. 2. Potential distribution of the conduction band edge of an asymmetrically doped DBQW structure (a) at vanishing external electric voltage and (b) at an external voltage corresponding to flatband condition in the barrier region. The arrows indicate the processes relevant for detector operation.

The observed systematic dependence of  $V_N$  on the position of the doping spikes strongly suggests that space-charge effects are of importance for the photovoltaic behavior. In Fig. 2(a), we have schematically plotted the potential distribution in an asymmetrically doped multiple DBQW structure for the case of zero external voltage. In this example, the left-hand side of the well is undoped, thus giving rise to a negative space-charge (negative curvature of the conduction band edge in Fig. 2) in this region caused by electrons in the lowest subband. Both the right-hand side of the well and the adjacent barrier region are assumed to be Si doped. Positive space charges arise (i) in the barrier region due to depletion of the dopants by electron capture into the well and (ii) at the right-hand part of the well because of the decay of the electron wave function towards the barrier layers. Here, vanishing external bias implies periodic boundary conditions for subsequent QWs. The electric dipole field across the well regions caused by these space charges therefore induces a field with opposite sign across the barrier regions.

The arrows in Fig. 2(a) illustrate the photoconduction mechanism in such a structure. Electrons which are optically excited from the lower to the upper subband of a QW (vertical arrows) have a finite probability to be emitted from the well before intersubband relaxation occurs. Due to the different relative height of the AIAs tunnel barriers with respect to the upper subband, the probability for electron emission towards the right-hand side of the well is expected to be larger than for emission to the left-hand side. Nevertheless, the space-charge field across the  $\text{Al}_{0.3}\text{Ga}_{0.7}\text{As}$  barrier layers gives rise to a net electron current towards the left since the majority of the emitted carriers relaxes back into the well located at the left-hand side of the barrier. The transport asymmetry caused by this back-relaxation process depends on temperature, on the precise values of the space-charge fields, and on the transport properties of the AIAs tunnel barriers at energies close to the  $\text{Al}_{0.3}\text{Ga}_{0.7}\text{As}$  band edge. The latter effect is not expected to be critical, since the AIAs barriers can be readily traversed via  $\Gamma$ - $X$  scattering processes. We note that the resulting space-charge induced asymmetry can both be enhanced<sup>9</sup> and compensated by appropriate thickness or compositional asymmetries of the tunnel barriers.

Figure 2(b) describes the situation for the case where the space-charge field across the  $\text{Al}_{0.3}\text{Ga}_{0.7}\text{As}$  layers is compensated by an external voltage  $V_{\text{ext}}$  such that the transport asymmetry of the photoexcited electrons is removed. This situation corresponds essentially to the experimental condition  $V_{\text{ext}} = V_N$ , i.e., to the condition of vanishing photocurrent. Emission of the photoexcited electrons from the QWs may still show some asymmetry due to the different barrier potentials on both sides of the well; this asymmetry, however, is compensated by very small changes of the bias, particularly at low temperatures.

To obtain a quantitative understanding of the dependence of  $V_N$  on the doping profile, we present a simple analysis of the variations in the space-charge distributions for different doping spike positions. We use the one-dimensional Poisson equation  $\partial F/\partial z = \rho/\epsilon$ , which relates the spatial derivative of the electric field  $F$  along the growth direction  $z$  to the space-charge density  $\rho(z)$  and the dielectric constant  $\epsilon = \epsilon_0\epsilon_r$ . For  $\rho/e = 2 \times 10^{18} \text{ cm}^{-3}$  and  $\epsilon_r = 13.18$  (Ref. 11), we obtain  $\rho/\epsilon = 27.5 \text{ kV/cm nm}$ , assuming for simplicity an abrupt transition from depleted to undepleted material. For the situation depicted in Fig. 2(b), the maximum space-charge field in the well region is  $F_{sc} = d_{sc}\rho/\epsilon$ , where  $d_{sc}$  is the width of the depleted layer. The distance (dipole width) between the positive and negative space charges is assumed to be  $d_d = 4 \text{ nm}$ , i.e., the nominal width of the doping spike. This results in a potential drop of  $V_d = d_d F_{sc}$  for each DBQW. For a detector with  $n$  DBQW periods, we thus obtain  $V_N = nV_d$ , which has to be checked experimentally.

An absolute verification of this relation cannot be carried out for the present samples since this would require a knowledge of the *actual* dopant distribution across the DBQW with sub-nm precision. However, since the samples were produced under identical growth conditions, the *relative positions* of the dopant distributions between the individual samples are expected to be identical to the intended ones, and to be the only change from sample to sample. According to the growth conditions, the depletion width  $d_{sc}$  should vary by 1.0 nm between sample 1 and sample 3, corresponding to a change in  $V_N$  of 0.55 V.

The upper inset of Fig. 1 shows the experimental dependence of  $V_N$  on the relative doping position, with the center-doped sample 2 taken as a reference. The measured change in  $V_N$  between samples 1 and 3 is 0.7 V, which is in reasonable agreement with the theoretical value. The deviation is presumably due to a redistribution of the accumulation space charge and/or nonrectangular doping profiles, both in the  $z$  direction, thus giving rise to an effective dipole width of  $d_d > 4 \text{ nm}$ .

If additional contributions to the photovoltage are ignored, extrapolation towards  $V_N = 0$  indicates a shift of the actual doping position by 2.3 nm (in growth direction) with respect to the intended position (see upper inset of Fig. 1). However, photovoltaic asymmetries can also arise from inequivalent interface roughnesses, compositional asymmetries, and inequivalent barrier thicknesses.<sup>9</sup> In ad-

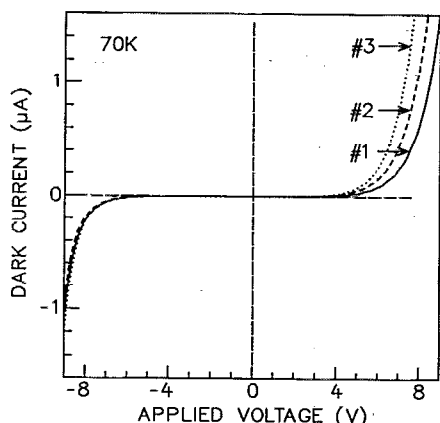


FIG. 3. Dark current vs applied voltage of the DBQW structures.

dition, dopant incorporation within the AlAs tunnel barriers may cause a modification of the tunneling characteristics. When taking into account these effects, the resulting dopant shift might be reduced. Dopant migration lengths on the order of 2 nm at a growth temperature of 580 °C are consistent with the results of an earlier study<sup>10</sup> of Si incorporation in intersubband detector structures.

The space-charge effect discussed here also explains a feature of the *dark current* which was observed in previous experiments, namely an asymmetry in the voltage dependence of the dark current which is *opposite* to that of the photocurrent.<sup>7,12</sup> Dark current versus voltage curves of the present samples are plotted in Fig. 3. Indeed, the dark current of each sample is larger for the bias polarity at which electron transport occurs in the growth direction (positive bias), indicating a preferential electron transport direction towards the top side of the DBQW structure. Such a discrepancy between photocurrent and dark current is not observed in photoconductive (i.e., symmetric) intersubband detectors, since a voltage-induced change of the excited-electron mean free path should influence the values of the photo- and dark currents in the same way. In this context, however, the explanation of the discrepancy is straightforward. We have shown previously<sup>8</sup> that the dark current in the present field regime is due to tunneling-assisted thermionic emission from the well into the adjacent  $\text{Al}_{0.3}\text{Ga}_{0.7}\text{As}$  layers. From Fig. 2 it can be seen that the activation energy for this emission process, which is essentially the difference between the lower subband energy and the  $\text{Al}_{0.3}\text{Ga}_{0.7}\text{As}$  band edge, is smaller for emission towards the top side than for emission towards the substrate side of the well, thus giving rise to a preferential carrier emission towards the top side. This explanation is further confirmed by the fact that the dark current asym-

metry increases for the increasing space-charge asymmetry in samples 1, 2, and 3. Finally, this increase is very pronounced at positive voltages while there is no significant effect at negative bias. In fact, if a dopant shift along the growth direction has occurred, the barrier energy on the bottom side of the QW (relative to the lowest subband) is expected to be less sensitive to the dopant position than that on the top side of the QW.

In conclusion, we have investigated the effect of space-charge asymmetries on the photovoltaic behavior of double barrier quantum well intersubband detectors. We found a drastic influence of the dopant position on the observed photocurrent asymmetry, which can be quantitatively explained in terms of space-charge effects. These results provide an understanding of (i) the physics of the transport mechanism giving rise to the photovoltaic asymmetry, and (ii) the different asymmetry observed for the dark current. It would be interesting to use this concept of photovoltaic intersubband detection, which presently works in the 3–5  $\mu\text{m}$  short-wavelength infrared, for further optimization of QW detectors in the 8–12  $\mu\text{m}$  regime.

The authors are grateful to J. Wagner and B. Dischler for helpful discussions and to H. Rupprecht for encouragement of this work. We would also like to thank J. Fleissner, C. Hoffmann, M. Hoffmann, and K. Räuber for diode processing, and to H. Biebl for absorption measurements. Thanks are due to the referee for relating the independence of the dark current at reverse bias with the dopant shift.

<sup>1</sup>B. F. Levine, C. G. Bethea, K. G. Glogovsky, J. W. Stayt, and R. E. Leibenguth, *Semicond. Sci. Technol.* **6**, C114 (1991).

<sup>2</sup>J. Y. Anderson and L. Lundqvist, in *Intersubband Transitions in Quantum Wells*, edited by E. Rosencher, B. Vinter, and B. Levine (Plenum, London, 1992), p. 1.

<sup>3</sup>E. Martinet, F. Luc, E. Rosencher, Ph. Bois, and S. Delaitre, *Appl. Phys. Lett.* **60**, 895 (1992).

<sup>4</sup>J. S. Park, R. P. G. Karunasiri, and K. L. Wang, *Appl. Phys. Lett.* **60**, 103 (1992).

<sup>5</sup>A. Köck, E. Gornik, G. Abstreiter, G. Böhm, M. Walther, and G. Weimann, *Appl. Phys. Lett.* **60**, 2011 (1992).

<sup>6</sup>H. C. Liu, *Appl. Phys. Lett.* **60**, 1507 (1992).

<sup>7</sup>H. Schneider, F. Fuchs, B. Dischler, J. D. Ralston, and P. Koidl, *Appl. Phys. Lett.* **58**, 2234 (1991).

<sup>8</sup>H. Schneider, P. Koidl, F. Fuchs, B. Dischler, K. Schwarz, and J. D. Ralston, *Semicond. Sci. Technol.* **6**, C120 (1991).

<sup>9</sup>J. D. Ralston, H. Schneider, D. F. G. Gallagher, K. Kheng, F. Fuchs, P. Bittner, B. Dischler, and P. Koidl, *J. Vac. Sci. Technol. B* **10**, 998 (1992).

<sup>10</sup>J. D. Ralston, H. Ennen, M. Maier, M. Ramsteiner, B. Dischler, P. Koidl, and P. Hiesinger, *Mater. Res. Soc. Symp. Proc.* **163**, 875 (1990).

<sup>11</sup>S. Adachi, *J. Appl. Phys.* **58**, R1 (1985).

<sup>12</sup>H. Schneider, K. Kheng, F. Fuchs, J. D. Ralston, B. Dischler, and P. Koidl, in *Intersubband Transitions in Quantum Wells*, edited by E. Rosencher, B. Vinter, and B. Levine (Plenum, London, 1992), p. 73; H. Schneider, K. Kheng, M. Ramsteiner, J. D. Ralston, F. Fuchs, and P. Koidl, *Appl. Phys. Lett.* **60**, 1471 (1992).